AAM (author's accepted manuscript) Eur. J. Cell Biol. *89*:723-732, 2010

Phospholipids regulate localization and activity of mDia1 formin

Nagendran Ramalingam[1,2,*], Hongxia Zhao[3], Dennis Breitsprecher[4], Pekka Lappalainen[3], Jan Faix[4] and Michael Schleicher[1§]

[1]Institute for Anatomy and Cell Biology, Ludwig-Maximilians-Universitaet, 80336 Muenchen, Germany, [2]Center for Biochemistry I, Center for Molecular Medicine Cologne (CMMC) and Cologne Excellence Cluster on Cellular Stress Responses and Aging-Associated Diseases (CECAD), Universitaet zu Koeln, 50931 Koeln, Germany, [3]Institute of Biotechnology, PO Box 56, 00014 University of Helsinki, Finland, [4]Institute for Biophysical Chemistry, Hannover Medical School, 30623 Hannover, Germany

Running title: Phospholipids regulate mDia1

* Current address: Department of Pathology and Cell Biology, Columbia University, New York, NY 10032, USA

§ Corresponding author:
Prof. Dr. Michael Schleicher
Institute for Anatomy and Cell Biology
LMU Muenchen
Schillerstr.42, 80336 Muenchen, Germany,
Telephone: +49-89-2180-75876, Fax: +49-89-2180-75004,
E-mail: schleicher@lrz.uni-muenchen.de

ABSTRACT

Diaphanous-related formins (DRFs) are large multi-domain proteins that nucleate and assemble linear actin filaments. Binding of active Rho family proteins to the GTPase-binding domain (GBD) triggers localization at the membrane and the activation of most formins if not all. In recent years GTPase regulation of formins has been extensively studied, but other molecular mechanisms that determine subcellular distribution or regulate formin activity have remained poorly understood. Here, we provide evidence that the activity and localization of mouse formin mDia1 can be regulated through interactions with phospholipids. The phospholipid-binding sites of mDia1 are clusters of positively charged residues in the N-terminal basic domain (BD) and at the C-terminal region. Upon binding to the lipid bilayer the N-terminal region of mDia1 induces strong clustering of phosphatidylinositol-4,5-bisphosphate (PIP_2) and subsequently inserts into the membrane bilayer thus anchoring mDia1 to the reconstituted plasma membrane. In addition, an interaction of phospholipids with the C-terminal region of mDia1 causes a drastic reduction of its actin filament assembly activity. Our data suggest that the N-terminal phospholipid-binding sites help to anchor formins at the plasma membrane, and the interaction with phospholipids in the C-terminus functions as a switch for transient inactivation.

KEYWORDS

Formins, mDia, actin-binding proteins, actin polymerizatiom and phospholipids.

INTRODUCTION

Formins are ubiquitous and highly conserved multi-domain proteins that nucleate and elongate linear actin filaments by insertional incorporation of monomers to the filament barbed ends (Faix and Grosse, 2006; Kovar and Pollard, 2004; Pollard, 2007). The proline-rich formin homology domain 1 (FH1) recruits profilin-actin complexes for filament elongation (Kovar et al., 2006; Paul and Pollard, 2008; Romero et al., 2004) which is accomplished by the adjacent FH2 domain (Higashida et al., 2004; Shimada et al., 2004; Xu et al., 2004). Members of the family of Diaphanous-related formins (DRF) fold on themselves and are thus intrinsically inactive by virtue of additional regulatory sequences located in the N- and C-terminal regions of these proteins (Alberts, 2001; Li and Higgs, 2005; Wallar et al., 2006). Binding of activated small Rho family GTPases such as RhoA to the GTPase-binding domain (GBD) releases this intra-molecular inhibition by disrupting the interaction between the C-terminal Diaphanous-auto-regulatory domain (DAD) and the N-terminal Diaphanous-inhibitory domain (DID) (Brandt et al., 2007; Nezami et al., 2006; Otomo et al., 2005; Rose et al., 2005; Wallar and Alberts, 2003). The dimerization domain (DD) is sufficient to dimerize the N-terminal region even without the adjacent coiled-coil (CC) region, while a short linker within the FH2 domain facilitates the dimerization of the C-terminus (Otomo et al., 2005; Xu et al., 2004).

Although the auto-inhibition and the GTPase signaling in mammalian DRF's regulation are well understood, other mechanisms that control e.g. their localization are largely unknown. Formins are often enriched at the plasma membrane (Seth et al., 2006) or in filopodial tips (Block et al., 2008; Schirenbeck et al., 2005). The molecular basis of this distribution is still not entirely understood and the interaction with a membrane-associated GTPase is apparently not the only mechanism (Copeland et al., 2007; Seth et al., 2006; Zaoui et al., 2008). CLIP170 and IQGAP1 have been described to recruit mDia1 to the phagocytic cup (Brandt et al., 2007; Lewkowicz et al., 2008), and FMNL1 inserts into membranes after being myristoylated at the N-terminus (Han et al., 2009). Additional types of formin regulation have been reported for yeast formins. Budding yeast Bud6 interacts directly with the DAD of Bni1 and stimulates its activity, whereas Bud14 inhibits the activity of the formin Bnr1 by displacing it from the growing filament barbed end (Chesarone et al., 2009; Moseley et al., 2004). Furthermore, the N-terminal region and the FH1FH2 domain of Cdc12p are obviously important for its localization to the contractile ring (Yonetani et al., 2008).

Here we report that the mouse DRF mDia1 can be anchored to the plasma membrane through an interaction of its N-terminal basic domain (BD) with phospholipids. Furthermore, the C-terminal region of mDia1 also binds PIP_2 and this interaction inhibits mDia1-induced actin filament assembly. Thus our observations suggest that the activity and localization of mDia1 are two distinct phenomena.

MATERIALS AND METHODS

Cell culture and transfection

NIH 3T3 fibroblasts were maintained in DMEM with 10% FBS and 2 mM glutamine. Cells were transfected with 2 µg plasmid DNA using LipofectAMINE 2000 (Invitrogen). Microscopy was performed essentially as described (Schirenbeck et al., 2005). Briefly, 10 hours after transfection live cells expressing GFP-fusion proteins were imaged in phosphate buffer using a LSM 510 Meta (Zeiss, Germany) at 30°C.

Plasmids

For cloning and expression of EGFP-mDia1, the entire gene and truncated fragments (ΔDAD – amino acids #1-1179 and ΔBDΔDAD #61-1179) were PCR amplified from mouse cDNA and inserted into the BglII/SalI sites of pEGFP-C1 (Clontech). For the expression of mDia1, mDia2, mDia3 and the RhoA(V14) constructs in *E. coli*, appropriate inserts were amplified by PCR and cloned into pGEX-6P-1 or pGEX-4T-1(GE Healthcare). Hot-Start Phusion polymerase (Finnzymes) was used for the site directed mutagenesis experiments.

Protein expression and purification

ArcticExpress^{TM} RP competent cells (Stratagene) were transformed with GST-mDia1 full-length, GST-mDia1ΔDAD (amino acids #1-1179), GST-mDia1ΔBDΔDAD (amino acids #61-1179), GST-mDia1FH1FH2DAD (amino acids #702-1255), GST-mDia2FH1FH2DAD (amino acids #521-1171), GST-mDia3FH1FH2DAD (amino acids #586-1102) and GST-mDia1DAD (amino acids #1180-1255). The cells were grown to mid-log at 30˚ C and subsequently expression was induced with 0.5 mM IPTG for 15 hours at 10˚C. The N-terminal constructs of mDia1 and GST-RhoA(V14) were expressed in BL21RIL cells (Stratagene) at 16˚C for 10 hours after induction at an optical density of 0.6 at 600 nm. Purification of GST and fusion proteins was done as described (Faix et al., 1998). The GST tag was cleaved off by incubating GST-RhoA(V14), GST-mDia1DAD, GST-mDia1N570, GST-mDia1Δ12-42N570, GST-mDia1N46, GST-mDia1 FH1FH2DAD with PreScission protease (GE Healthcare) or thrombin (Novagen) in PBS supplemented with 1 mM DTT at 4˚C for 10 hours. Free GST and PreScission protease were then removed by passing the solution over a glutathione-agarose column; thrombin was removed by benzamidine agarose resin. All other proteins were used as GST fusions in the biochemical assays.

Preparation of large unilamellar vesicles (LUVs)

Diphenylhexatriene (DPH) was from Invitrogen and bodipy-TMR-PIP_2 was purchased from Echelon (Salt Lake City, Utah). 1-palmitoyl-2-{6-[(7-nitro-2-1,3-benzoxadiazol-4-yl)amino]-hexanoyl}-*sn*-glycero-3-phosphoserine (NBD-PS), 1-palmitoyl-2-oleoyl-*sn*-glycero-3-phosphatidylcholine (POPC), 1-palmitoyl-2-oleoyl-*sn*-glycero-3-phosphatidylethanol-amine (POPE), 1-palmitoyl-2-oleoyl-*sn*-glycero-3-phosphatidylserine (POPS), and L-α-phosphatidylinositol-4,5-bisphosphate (PIP_2) were purchased from Avanti Polar Lipids (Alabaster, AL). Lipids in desired concentrations were mixed, dried under a stream of nitrogen and hydrated in 20 mM Hepes, pH 7.5, 100 mM NaCl to yield multilamellar vesicles in a lipid concentration of 1 mM. To obtain unilamellar vesicles, vesicles were extruded through a polycarbonate filter (100 nm pore size) using a mini-extruder (Avanti Polar Lipids). One should take into account that experiments with lipid vesicles can not directly reflect the situation at a biological membrane. In a large PC vesicle dotted with many PIP_2 molecules the geometry of the vesicle will allow only a few acidic lipid molecules to interact with a target protein. Consequently, the given PIP_2 concentration for the preparation of LUVs is only a very crude approximation to physiological conditions and requires very detailed titration experiments for exact binding characteristics. The inner leaflet of the plasma membrane contains in a normal cell (of all phospholipids) only 0.5-1% PIP_2 but 25 - 35% of PS (Lemmon, 2008; McLaughlin and Murray, 2005). Therefore, the lipid binding data in this study focus more on qualitative than quantitative analyses.

Fluorescence spectroscopy experiments

Phospholipid clustering and membrane insertion experiments were performed essentially as described (Saarikangas et al., 2009). Briefly, fluorescence spectra and DPH anisotropy were measured with a Perkin-Elmer LS 55 spectrometer with both emission and excitation band passes set at 10 nm. Spectra were corrected for the contribution of light scattering in the presence of

vesicles. NBD-PS fluorescence was excited at 470 nm and the emission spectra were recorded from 490 nm to 560 nm with band passes set at 5 nm and 10 nm, respectively. Bodipy-TMR-PIP_2 fluorescence was excited at 547 nm and the emission spectra were recorded from 555 to 600 nm in the presence of different concentrations of proteins. The percentage of quenching was calculated using the following equation:

% quenching = $(1-F/F_0)\times100$,

where F is the fluorescence intensity in the presence of protein or liposomes, and F_0 is the fluorescence intensity in the absence of protein or liposomes. Fluorescence anisotropy of DPH was measured by including DPH into liposomes at $X = 0.002$. Fluorescence anisotropy for DPH was measured with excitation at 360 nm and emission at 450 nm, using 10 nm bandwidths. The lipid concentration used was 40 µM for DPH anisotropy, NBD-PS, and bodipy-TMR-PIP_2 fluorescence measurements.

In vitro actin polymerization assays

Actin from skeletal muscle was purified as described (Spudich and Watt, 1971). Actin polymerization was measured by fluorescence spectroscopy with pyrene-labeled actin (Schirenbeck et al., 2006; Schirenbeck et al., 2005) and performed in a buffer containing 10 mM imidazole, 2 mM $MgCl_2$, 0.2 mM $CaCl_2$, 1 mM Na_2ATP, and 50 mM KCl (pH 7.2).

TIRF assays

Time-lapse evanescent wave fluorescence microscopy was performed as described (Breitsprecher et al., 2008). Briefly, the assembly of 1 µM ATP-actin and 0.3 µM Alexa-Fluor-488-labelled ATP-actin in TIRF buffer (10 mM imidazole (pH 7.4), 50 mM KCl, 1 mM $MgCl_2$, 1 mM EGTA, 0.2 mM ATP, 50 mM DTT, 15 mM glucose, 20 µg/ml catalase, 100 µg/ml glucose oxidase and 0.5% methylcellulose) on cover slips coated with 10 nM N-ethlymaleimide (NEM) myosin II and formins (in the presence or absence of liposomes). Images from an Olympus IX-81 inverted microscope were captured every 10 or 15 s with exposures of 200 or 500 ms with a Hamamatsu ER C8484 CCD camera (Hamamatsu Corp., Bridgewater, NJ).

Cosedimentation assay

Small unilamellar liposomes were made and concentrations calculated as described (Prehoda et al., 2000) with minor modifications. Briefly, L-α-phosphatidylcholine (PC), L-α-phosphatidylserine (PS) and PIP_2 were dissolved separately in chloroform/methanol/water (20:9:1) and dried under nitrogen. The lipids were then resuspended in 20 mM HEPES pH 7.3 and 150 mM NaCl followed by sonication until the solution became clear. At indicated ratios the lipids were mixed and sonicated again just prior to usage. All lipids were purchased from Avanti Polar Lipids (Alabaster, AL, USA).

Cosedimentation assays were performed by mixing ~3 µM protein and ~50 µM phospholipid vesicles at indicated ratios in 20 mM HEPES pH 7.3, 150 mM NaCl, 2 mM EGTA (total assay volume 50 µl), incubation at 25°C for 60 min, and centrifugation at 10,000 g for 30 min at room temperature. The pellets were washed once with 100 µl of the reaction buffer. Subsequently, the volumes of the pellets and supernatant fractions were normalized and analyzed by SDS-PAGE and Coomassie blue staining (Eichinger and Schleicher, 1992).

RESULTS

The N-terminal basic region of mDia1 interacts directly with liposomes.

The first 60 residues of mDia1 referred to as the basic domain (BD) harbor three clusters of positively charged residues encompassed by the amino acids #12-21, #35-42, and #47-54 (Figure 1A). A similar basic region is also present in mDia2 but not in mDia3. DAAM proteins contain

only a single poly-basic cluster close to the N-terminus (Figure 1B). To test whether the basic domain of mDia1 can interact with the negatively charged phospholipids such as PS and PIP_2, several truncation and deletion constructs were expressed as GST-fusion proteins and tested for their ability to co-sediment with lipid vesicles containing PC (phosphatidylcholine), PS (phosphatidylserine) and PIP_2. After cosedimentation, proteins from pellets (P) and supernatants (S) were analyzed by SDS-PAGE. The results revealed that the BD of mDia1 but not the other regions in the N-terminal region interacts with lipid vesicles containing both PS and PIP_2 (Figure 2A). Vesicles containing only PC showed no interaction with the BD, implying the requirement of negative charges for the binding of mDia1 with membranes (not shown).

To map the lipid-binding region within the BD (residues #1-46), the cosedimentation assays were repeated in the presence of the two mDia1-derived synthetic peptides A and B spanning either the first or the second basic amino acid clusters (Figure 1A). Both peptides (residues #12-21 and #35-42) could compete with N46 for liposomes containing PS and PIP_2. In a competition assay with the synthetic peptides the inhibitory effect of the second basic stretch turned out to be significantly higher than that of the first poly-basic cluster (Figure 2B). The construct (Δ12-42N570) that contained only the third poly-basic basic cluster did not interact with phospholipids (Figure 2A). Presumably due to the presence of glutamic acid residues within the third poly-basic cluster (residues #47-54) this region was dispensable for phospholipid interactions. We therefore assume that the first two poly-basic clusters act in a 'bipartite' manner.

The N-terminal region of mDia1 clusters PIP_2 and inserts into the membrane.

The binding of mDia1 BD to membranes was further investigated by fluorescence spectroscopy. The protein fragments tested were mDia1N570 (residues #1-570), mDia1Δ12-42N570 (residues #1-570 with a deletion of residues #12-46) and mDia1N46 (residues #1-46). In these assays, the fluorescent probes NBD-PS and bodipy-TMR-PIP_2 were applied for examining the binding of mDia1 N-terminus to PS and PIP_2, respectively, in Large Unilamellar Vesicles (LUV). mDia1 fragments induced quenching of NBD fluorescence, indicating binding to PS (Figure 3A). Membrane-binding of mDia1 fragments also induced quenching of bodipy fluorescence. Since bodipy has highly superimposable absorption and emission spectra it exhibits self-quenching when two or more molecules are brought together in close proximity. Thus, quenching is caused by the static and/or dynamic interaction of bodipy-TMR PIP_2 and indicates clustering of PIP_2 molecules by mDia1N570 (Figure 3B).

Although our results revealed that the mDia1N570 binds both to PS and PIP_2, it appears to interact with higher affinity with PIP_2 (Figure 3A and B). Deletion of residues 12 to 42 from the N-terminal mDia1 fragment diminished binding to PS and PIP_2 (Figure 3A and B). The peptide consisting of the first 46 residues bound strongly to both PS and PIP_2, suggesting that these amino acids are important for PS and PIP_2 binding (Figure 3A and B). However, the robust lipid-binding activity of N46 might not represent the actual situation as this fragment is likely to be structurally more simple compared to that of the construct mDia1N570.

To test if the BD-membrane interaction is just electrostatic or whether the N-terminus is capable of inserting into the membrane bilayer, we studied steady-state fluorescence anisotropy of 1,6-diphenyl 1,3,5-hexatriene (DPH). DPH readily diffuses into the hydrophobic core of a lipid bilayer without influencing the physical properties of the plasma membranes and can thus be used to monitor changes in the rotational diffusion of the fatty acyl chains in the lipid bilayer (Zaritsky et al., 1985). Interestingly, binding of mDia1N570 to the reconstituted plasma membrane caused a considerable increment in DPH anisotropy, indicating that this fragment

inserts into the lipid bilayer. Consistent with the sedimentation and lipid clustering data, the protein variant lacking residues 12-42 (Δ12-42N570) with reduced PS and PIP_2-binding affinity inserted less efficiently into the lipid bilayer as compared to the wild type N-terminal fragment. Moreover, insertion of the mDia1 fragment N570 into the lipid bilayer was enhanced in the presence of PIP_2, suggesting that the interaction with PIP_2 facilitates membrane insertion. The N-terminal 46 amino acid peptide (N46) did not cause detectable changes in DPH anisotropy which implies that the BD is not directly involved in membrane insertion (Figure 3C and D). However, it could play a pivotal role in facilitating the insertion of other regions of mDia1 by first attaching the protein to the membrane through electrostatic interactions with negatively charged lipids of the plasma membrane. Essentially, our data indicate that there is a substantial plasma membrane-BD interaction beyond the attraction for negative charges.

The basic domain (BD) is essential for targeting mDia1 to the plasma membrane.

In a previous report the authors showed that the complete N-terminus of mDia1 up to the CC domain was localized at the plasma membrane and a point mutation in the GBD that renders defective Rho binding abolished membrane interaction only partially (Seth et al., 2006). This triggered the claim for GTPase-independent membrane-binding activities of mDia1. Therefore, we dissected the mDia1 N-terminus also in vivo by expressing wild type and truncated mDia1 constructs as enhanced green fluorescent protein (EGFP) fusions (Figure 4A) in mouse NIH 3T3 fibroblasts and found, as expected, auto-inhibited full-length mDia1 (EGFP-mDia1FL) distributed uniformly throughout the cell (Figure 4B, left panel).

Consequently, expression of a constitutively active construct that still contained the BD but lacked the DAD (EGFP-mDia1ΔDAD) was recruited to the plasma membrane (Figure 4B, middle panel), and another constitutively active construct without the BD (EGFP-mDia1ΔBDΔDAD) lost its pronounced association with the plasma membrane again (Figure 4B, right panel). In actin polymerization assays both mDia1ΔDAD and mDia1ΔBDΔDAD showed comparable activities (Figure S1). So the distinct cellular distribution is not the result of differences in biochemical activity but depends at least in part on the lipid-binding. A strong accumulation of both EGFP-mDia1ΔDAD and EGFP-mDia1ΔBDΔDAD constructs in filopodial tips (Figure 4B) suggests that the localization to filopodial tips can not be the result of an interaction with the tip membrane.

Given that the four independent constructs EGFP-mDia1BD, EGFP-mDia1GBD, EGFP-mDia1BD-GBD and EGFP-mDia1ΔBDΔDAD (Figure 4B and not shown) failed to localize to the plasma membrane an involvement of multiple signals is quite obvious. In less than 15% of all cells expressing EGFP-mDia1ΔBDΔDAD, the protein still accumulated at the plasma membrane (Figure 4C, right column). The most reasonable explanations for this small subpopulation are membrane recruitment through other formin domains and/or the formation of hetero-dimers between the endogenous DID and the DAD of mutated versions of mDia1. Since, mDia2 contains a similar basic region in its N-terminus (Figure 1B), this type of membrane recruitment employed by the first two basic clusters may also be used by other formins.

PIP_2-BD interaction does not enhance Rho-induced activity of mDia1 but PIP_2 inhibits the activity of FH1FH2DAD.

The domain architecture of mDia1 is reminiscent of N-WASP whose auto-inhibition is completely relieved by both Cdc42 and PIP_2 (Higgs and Pollard, 2000; Prehoda et al., 2000; Rohatgi et al., 2000). Therefore, in vitro actin polymerization assays were carried out to decipher the role of PIP_2 in the regulation of mDia1 activity. The tool for this assay was the artificial inhibition of FH1FH2DAD by N570. The two proteins fragments bind to each other in the same

fashion as it is the case in auto-inhibited full-length formin. This inter-molecular DID/DAD interaction was only partially abolished by an addition of constitutively active RhoA(V14). Assuming that PIP_2 will synergistically activate formin along with RhoA(V14), liposomes containing PC/PS/PIP_2 were added to the cocktail of protein mixtures containing FH1FH2DAD, N570 and RhoA(V14). In contrast to our expectations, an inhibition in the formin activity was evident (Figure S2). This result clearly suggests that (i) the BD-PIP_2 interaction did not influence the formin activity synergistically with RhoA, and (ii) another phospholipid-binding and inhibitory region in mDia1 must be present in the C-terminal half of the molecule encompassing the FH1FH2DAD.

PIP_2 negatively regulates the actin assembly mediated by mDia1FH1FH2DAD.

To get further insights into the effects of PIP_2 on formin-mediated actin assembly in vitro Total Internal Reflection Fluorescence (TIRF) microscopy was employed to evaluate the impact of PIP_2 on formin-mediated actin nucleation and elongation at the single filament level. mDia1-associated actin filaments were previously shown to grow indistinguishably from the actin control in the absence of profilin. Although profilin enhances mDia1-mediated actin assembly about 5-fold (Kovar et al., 2006), we could not use profilin in our experimental set-up since PIP_2 inhibits the formation of the profilin-actin complexes (Lassing and Lindberg, 1985). Therefore, glass slides were first coated with GST-formin constructs and low amounts of N-ethylmaleimide (NEM)-myosin II. After addition of actin monomers the formation of actin filaments was then analyzed in a 100 μm^2 area. Formin-mediated actin assembly was scored by one of the following three criteria:

(i) the appearance of "buckling" filaments due to the insertional assembly of monomers at the barbed ends while the filaments were also attached to the substrate by NEM-myosin II (see schematic representation in Figure 5B),

(ii) the capture and subsequent elongation of spontaneously growing actin filament barbed ends by formins, also resulting in filament buckling, and

(iii) a bright fluorescence at the growing barbed ends bound to immobilized formins, paralleled by a fading signal towards the pointed end due to bleaching.

The regulation of mDia1 activity was tested in the presence of RhoA and phospholipids (Figure 5A and C). Auto-inhibited full-length mDia1 (mDia1-FL) alone exhibited only a basal activity accounting for less than about 5% of active formins. An addition of constitutively active RhoA(V14) enhanced mDia1-mediated actin assembly up to a maximum of over 100 active formins in the area of interest. Incubation of PIP_2 containing vesicles with RhoA-activated mDia1, however, drastically impaired this activity. RhoA-activated full-length mDia1 lost its actin assembly activity after the addition of 150 nM PIP_2 in PC/PS/PIP_2 vesicles. The constitutively active C-terminal fragment encompassing only mDia1FH1FH2DAD was similarly inhibited by PC/PS/PIP_2 vesicles, i.e. the BD in mDia1-FL does not contribute to this inhibition. An examination of mDia1FH1FH2DAD (residues #702-1255) by TIRF microscopy revealed that induced filament growth was almost completely inhibited by the addition of PIP_2 containing vesicles (Figure 5D and E). Spontaneous actin assembly in the absence of formin was not altered by PIP_2 (not shown).

Actin assembly was also inhibited in the presence of PIP_2 if one used the formin isoforms mDia2FH1FH2DAD and mDia3FH1FH2DAD (Figure S3). This profound effect of PIP_2 on mDia-mediated actin assembly renders PIP_2 a potent inhibitor of mDia formins. Since neither filament nucleation nor the capture of spontaneously growing filaments was observed in the presence of PIP_2, we hypothesize that this acidic lipid entirely blocks the interaction of the

formins with actin. Inhibition of actin polymerization by PIP_2 was also tested by fluorescence spectroscopy using large unilamellar liposomes. Titrations with different ratios of PC/PIP_2 (96:4, 90:10, 80:20, and 70:30) further demonstrated that PIP_2 inhibited formin-induced actin assembly in a dose-dependent manner. Figure 6A shows a representative experiment with PC/PIP_2 ratios of 70:30. An interaction of PIP_2 with certain actin-binding proteins was frequently described in recent years whereas actin itself was never a target. (switched order of the next 2 par.)

mDia1FH1FH2DAD clusters PIP_2 and inserts into reconstituted membranes.

To understand the mechanism of mDia1 negative regulation by phospholipids we investigated the mDia1FH1FH2DAD-phospholipid interaction using fluorescent lipid probes. As described above for the N-terminal mDia1 fragments, bodipy-TMR-PIP_2 was used to explore the membrane binding ability of mDia1FH1FH2DAD. Interestingly, our data revealed that FH1FH2DAD binds strongly to PIP_2-rich membranes (Figure 6B) which is consistent with our previous observations that increasing amounts of PIP_2 in the liposome mixture resulted in better inhibition (Figure 6). The bodipy-TMR-PIP_2 assay demonstrated that FH1FH2DAD also clustered PIP_2 upon binding to reconstituted membranes. DPH anisotropy measurements unequivocally indicated that like N570, FH1FH2DAD also inserted into the membrane containing PIP_2 or PS (Figure 6C). It is, however, not clear why PS-containing liposomes lacking PIP_2 did not inhibit the actin assembly mediated by FH1FH2DAD of mDia1 or mDia2 or mDia3 FH1FH2DAD (not shown and Figure S3 A and B). One possibility is that a lipid with a more specific head group and charge density is required for negative regulation but not for the electrostatic interactions per se. Remarkably, the C-terminal fragment encompassing the FH1FH2DAD inserted more efficiently than the N-terminus of mDia1.

The C-terminus of mDia1 harbors more than one PIP_2-binding site.

The intra-molecular interaction of DID and DAD was previously shown to be crucial for auto-inhibition of formins in vitro and in vivo (Lammers et al., 2005; Wallar et al., 2006). The inhibitory activity of PIP_2, however, employs a different mechanism and we hypothesized that the extreme C-terminus of mDia1 encompassing the DAD of mDia1 might at least in part be responsible for the interaction with PIP_2. In agreement with this assumption, addition of an excess of mDia1DAD (residues #1180-1255) relieved PIP_2-mediated inhibition of the mDia1FH1FH2DAD fragment in a dose-dependent manner (Figure S4). This confirmed that the C-terminus spanning the DAD is not only crucial for auto-inhibition of full-length formin but also for the negative regulation of an active mDia1 by PIP_2. First attempts to map motifs that are important for the interaction between phospholipids and mDia1FH1FH2DAD by mutating the conserved poly-basic residues to alanine showed that point mutations in DAD and in the mDia1FH1FH2 domain reduced clustering of PIP_2. Consistently, the nucleating activity of a construct lacking the DAD (mDia1FH1FH2) was also reduced by PIP_2 suggesting that more than one lipid-binding site is present within the FH1FH2 domain and the very C-terminal region (not shown).

DISCUSSION

Formins have been reported to target themselves to specific subcellular compartments by various mechanisms (Brandt et al., 2007; Copeland et al., 2007; Lewkowicz et al., 2008; Seth et al., 2006; Yonetani et al., 2008; Zaoui et al., 2008). In the present study we have demonstrated that the BD of mDia1 directly interacted with membrane phospholipids and this interaction is required for the targeting of mDia1 to the plasma membrane. Presumably this type of membrane recruitment is adapted by other DRF family members including mDia2 that possesses a similar

BD. Our steady state fluorescence spectroscopy data imply that the binding of mDia1 BD to phospholipids is not just an electrostatic interaction between the positively charged BD and the negatively charged lipids but could involve an additional interaction between hydrophobic protein regions with the lipid acyl chains in the membrane. Since both the first and the second basic clusters of mDia1 directly interacted with phospholipids independent of each other, they might work in a bipartite manner. Accordingly, the subcellular distribution of constitutively active DAAM1 (ΔDAD), which contains only one basic stretch in its N-terminus (Figure 1B) was recently shown to be entirely cytoplasmic (Liu et al., 2008). The finding corroborates our hypothesis that a single basic cluster such as the one present in DAAM1 may not be sufficient for phospholipid interaction and eventually membrane targeting. In addition, we also identified lipid-binding motifs at the C-terminus of mDia formins including mDia1, mDia2 and mDia3 as targets for membrane lipids. It is tempting to speculate that also these homologous motifs transiently inhibit formin activity upon binding to membrane lipids and thus circumvent the auto-inhibitory switch between inactive (closed) and active (open) conformations. The activities of mDia formins on the microtubule (MT) cytoskeleton are also mediated by FH2 domains. So it would be interesting to see if the regulation of MT is also affected by PIP_2 although the function of mDia on the actin and MT cytoskeleton can be segregated (Bartolini et al., 2008).

An important feature of actin dynamics in migrating cells is the need of filament elongation directly at the plasma membrane. Consequently, the majority of the filaments is not distributed randomly but rather in a polarized fashion with the fast growing barbed ends pointing towards the membrane and in parallel to the direction of movement. Formins are dimers, which can bind to the barbed end, add hand-over-hand actin monomers and, if they harbor the appropriate domain, stay bound to the plasma membrane. In a previous report, Rosen and coworkers showed that the complete N-terminus of mDia1 (amino acids # 1-570) was localized at the plasma membrane (Seth et al., 2006). However, the inactivation of GBD by a point mutation abolished membrane attachment only partially suggesting a more sophisticated mechanism and a membrane binding activity beyond the GBD. The discovery of an N-terminal region rich in basic residues (the BD) indicated the importance of BD-phospholipid interactions not only for plasma membrane recruitment but also for membrane insertion of active mDia1.

Our study in relation to published data indicates the cooperation among GBD, BD and DID. First of all, a membrane-bound GTPase opens the closed formin conformation by interaction with GBD (Li and Higgs, 2005; Rose et al., 2005), secondly the BD accomplishes the actual interaction with the negatively charged phospholipids PS/PIP_2 in the plasma membrane and finally the contact of DID to the scaffolding protein IQGAP strengthens the interaction between plasma membrane and the N-terminus of formin (Brandt et al., 2007). Thus a failure in any one of the signals will result in mislocalized mDia1.

The activity of potent actin nucleators has to be regulated differentially at independent levels. The inhibition of an active full-length mDia1 by PIP_2 occurs obviously after the protein has been activated by the GTP-bound RhoA upon a stimulus at the plasma membrane. The binding of mDia1 by RhoA opens the auto-inhibited structure and mDia1 attaches to the plasma membrane via its BD, maintaining its open conformation and nucleating filament formation. Possibly, the actin filaments grow until the C-terminus of formin reaches the plasma membrane. The C-terminus of formin then clusters PIP_2 and inserts into the lipid bilayer which leads to inhibition of actin filament elongation. The hydrolysis of PIP_2, i.e. the action of an entirely different signalling cascade, could reactivate the nucleating activity of the formin which is already present at the membrane in an open but inactivated conformation. The model in Figure 7 represents a

working hypothesis that is based (i) on well known formin activities (e.g. auto-inhibition, regulation by GTPases, domain characteristics), (ii) on our new findings (membrane association via interaction with lipids at the N-terminus, inhibition by lipids at the C-terminus), and (iii) predicted activities that have to be confirmed experimentally in the future (e.g. transient nucleating activities at the membrane).

The most prominent and best studied machineries driving the nucleation of actin filaments in vertebrate cells are formins and the Arp2/3-complex (Mattila and Lappalainen, 2008). The latter requires activation by so-called nucleation promoting factors such as neuronal Wiskott-Aldrich syndrome protein (N-WASp) (Stradal et al., 2004). Like formins, N-WASp or WASp are folded in an auto-inhibited conformation (Kim et al., 2000; Seth et al., 2006). The simultaneous binding of active Cdc42 and PIP_2 to the GTPase-binding domain (GBD) and to a basic region, respectively, relieves auto-inhibition of N-WASp or WASp completely, allows subsequent activation of the Arp2/3 complex and increased actin nucleation synergistically (Higgs and Pollard, 2000; Prehoda et al., 2000). The multi-domain architecture, auto-inhibition, the small GTPase and phospholipid signalling are all reminiscent of the DRF regulation. It is intriguing that the two key nucleators in the actin system are conversely regulated. In this scenario local changes of PIP_2 concentrations upon signal transduction could trigger either the formation of lamellipodial actin networks by Arp2/3 or the generation of linear actin structures by formins. Through this first formin-phospholipid study an unexplored direction is now revealed that aims at PIP_2 as a regulator for localization as well as activity of mDia1 and possibly its isoforms.

ACKNOWLEDGEMENTS

The authors thank Drs. A. Wittinghofer (MPI Dortmund) for the mDia1 cDNA clone, W. Tegge (Helmholtz Centre for Infection Research, Braunschweig) for providing mDia1 synthetic peptides, and D. Rieger, R. Allam and D. Kumar for excellent technical advice. We also thank S. Koehler and Dr. A. Bausch (TU Muenchen) for help with preparation of LUVs for in vitro actin polymerization assays. This work was supported by grants from the Elite Network Bavaria (to N.R), the Deutsche Forschungsgemeinschaft (to M.S. and J.F.), and grants from the Academy of Finland (to HZ and PL), the Sigrid Juselius Foundation and the Biocenter Helsinki (to PL).

REFERENCES

Alberts, A. S. (2001). Identification of a carboxyl-terminal diaphanous-related formin homology protein autoregulatory domain. *J Biol Chem* 276, 2824-30.

Bartolini, F., Moseley, J. B., Schmoranzer, J., Cassimeris, L., Goode, B. L. and Gundersen, G. G. (2008). The formin mDia2 stabilizes microtubules independently of its actin nucleation activity. *J Cell Biol* 181, 523-36.

Block, J., Stradal, T. E., Hanisch, J., Geffers, R., Kostler, S. A., Urban, E., Small, J. V., Rottner, K. and Faix, J. (2008). Filopodia formation induced by active mDia2/Drf3. *J Microsc* 231, 506-17.

Brandt, D. T., Marion, S., Griffiths, G., Watanabe, T., Kaibuchi, K. and Grosse, R. (2007). Dia1 and IQGAP1 interact in cell migration and phagocytic cup formation. *J Cell Biol* 178, 193-200.

Breitsprecher, D., Kiesewetter, A. K., Linkner, J., Urbanke, C., Resch, G. P., Small, J. V. and Faix, J. (2008). Clustering of VASP actively drives processive, WH2 domain-mediated actin filament elongation. *Embo J* 27, 2943-54.

Chesarone, M., Gould, C. J., Moseley, J. B. and Goode, B. L. (2009). Displacement of formins from growing barbed ends by bud14 is critical for actin cable architecture and function. *Dev Cell* 16, 292-302.
Copeland, S. J., Green, B. J., Burchat, S., Papalia, G. A., Banner, D. and Copeland, J. W. (2007). The diaphanous inhibitory domain/diaphanous autoregulatory domain interaction is able to mediate heterodimerization between mDia1 and mDia2. *J Biol Chem* 282, 30120-30.
Eichinger, L. and Schleicher, M. (1992). Characterization of actin- and lipid-binding domains in severin, a Ca(2+)-dependent F-actin fragmenting protein. *Biochemistry* 31, 4779-87.
Faix, J., Clougherty, C., Konzok, A., Mintert, U., Murphy, J., Albrecht, R., Muhlbauer, B. and Kuhlmann, J. (1998). The IQGAP-related protein DGAP1 interacts with Rac and is involved in the modulation of the F-actin cytoskeleton and control of cell motility. *J Cell Sci* 111 (Pt 20), 3059-71.
Faix, J. and Grosse, R. (2006). Staying in shape with formins. *Dev Cell* 10, 693-706.
Han, Y., Eppinger, E., Schuster, I. G., Weigand, L. U., Liang, X., Kremmer, E., Peschel, C. and Krackhardt, A. M. (2009). Formin-like 1 (FMNL1) is regulated by N-terminal myristoylation and induces polarized membrane blebbing. *J Biol Chem* 284, 33409-17.
Higashida, C., Miyoshi, T., Fujita, A., Oceguera-Yanez, F., Monypenny, J., Andou, Y., Narumiya, S. and Watanabe, N. (2004). Actin polymerization-driven molecular movement of mDia1 in living cells. *Science* 303, 2007-10.
Higgs, H. N. and Pollard, T. D. (2000). Activation by Cdc42 and PIP(2) of Wiskott-Aldrich syndrome protein (WASp) stimulates actin nucleation by Arp2/3 complex. *J Cell Biol* 150, 1311-20.
Kim, A. S., Kakalis, L. T., Abdul-Manan, N., Liu, G. A. and Rosen, M. K. (2000). Autoinhibition and activation mechanisms of the Wiskott-Aldrich syndrome protein. *Nature* 404, 151-8.
Kovar, D. R., Harris, E. S., Mahaffy, R., Higgs, H. N. and Pollard, T. D. (2006). Control of the assembly of ATP- and ADP-actin by formins and profilin. *Cell* 124, 423-35.
Kovar, D. R. and Pollard, T. D. (2004). Insertional assembly of actin filament barbed ends in association with formins produces piconewton forces. *Proc Natl Acad Sci U S A* 101, 14725-30.
Lammers, M., Rose, R., Scrima, A. and Wittinghofer, A. (2005). The regulation of mDia1 by autoinhibition and its release by Rho*GTP. *Embo J* 24, 4176-87.
Lassing, I. and Lindberg, U. (1985). Specific interaction between phosphatidylinositol 4,5-bisphosphate and profilactin. *Nature* 314, 472-4.
Lemmon, M. A. (2008). Membrane recognition by phospholipid-binding domains. *Nat Rev Mol Cell Biol* 9, 99-111.
Lewkowicz, E., Herit, F., Le Clainche, C., Bourdoncle, P., Perez, F. and Niedergang, F. (2008). The microtubule-binding protein CLIP-170 coordinates mDia1 and actin reorganization during CR3-mediated phagocytosis. *J Cell Biol* 183, 1287-98.
Li, F. and Higgs, H. N. (2005). Dissecting requirements for auto-inhibition of actin nucleation by the formin, mDia1. *J Biol Chem* 280, 6986-92.
Liu, W., Sato, A., Khadka, D., Bharti, R., Diaz, H., Runnels, L. W. and Habas, R. (2008). Mechanism of activation of the Formin protein Daam1. *Proc Natl Acad Sci U S A* 105, 210-5.
Mattila, P. K. and Lappalainen, P. (2008). Filopodia: molecular architecture and cellular functions. *Nat Rev Mol Cell Biol* 9, 446-54.
McLaughlin, S. and Murray, D. (2005). Plasma membrane phosphoinositide organization by protein electrostatics. *Nature* 438, 605-11.

Moseley, J. B., Sagot, I., Manning, A. L., Xu, Y., Eck, M. J., Pellman, D. and Goode, B. L. (2004). A conserved mechanism for Bni1- and mDia1-induced actin assembly and dual regulation of Bni1 by Bud6 and profilin. *Mol Biol Cell* 15, 896-907.
Nezami, A. G., Poy, F. and Eck, M. J. (2006). Structure of the autoinhibitory switch in formin mDia1. *Structure* 14, 257-63.
Otomo, T., Otomo, C., Tomchick, D. R., Machius, M. and Rosen, M. K. (2005). Structural basis of Rho GTPase-mediated activation of the formin mDia1. *Mol Cell* 18, 273-81.
Paul, A. and Pollard, T. (2008). The role of the FH1 domain and profilin in formin-mediated actin-filament elongation and nucleation. *Curr Biol* 18, 9-19.
Pollard, T. D. (2007). Regulation of actin filament assembly by Arp2/3 complex and formins. *Annu Rev Biophys Biomol Struct* 36, 451-77.
Prehoda, K. E., Scott, J. A., Mullins, R. D. and Lim, W. A. (2000). Integration of multiple signals through cooperative regulation of the N-WASP-Arp2/3 complex. *Science* 290, 801-6.
Rohatgi, R., Ho, H. Y. and Kirschner, M. W. (2000). Mechanism of N-WASP activation by CDC42 and phosphatidylinositol 4, 5-bisphosphate. *J Cell Biol* 150, 1299-310.
Romero, S., Le Clainche, C., Didry, D., Egile, C., Pantaloni, D. and Carlier, M. F. (2004). Formin is a processive motor that requires profilin to accelerate actin assembly and associated ATP hydrolysis. *Cell* 119, 419-29.
Rose, R., Weyand, M., Lammers, M., Ishizaki, T., Ahmadian, M. R. and Wittinghofer, A. (2005). Structural and mechanistic insights into the interaction between Rho and mammalian Dia. *Nature* 435, 513-8.
Saarikangas, J., Zhao, H., Pykalainen, A., Laurinmaki, P., Mattila, P. K., Kinnunen, P. K., Butcher, S. J. and Lappalainen, P. (2009). Molecular mechanisms of membrane deformation by I-BAR domain proteins. *Curr Biol* 19, 95-107.
Schirenbeck, A., Arasada, R., Bretschneider, T., Stradal, T. E., Schleicher, M. and Faix, J. (2006). The bundling activity of vasodilator-stimulated phosphoprotein is required for filopodium formation. *Proc Natl Acad Sci U S A* 103, 7694-9.
Schirenbeck, A., Bretschneider, T., Arasada, R., Schleicher, M. and Faix, J. (2005). The Diaphanous-related formin dDia2 is required for the formation and maintenance of filopodia. *Nat Cell Biol* 7, 619-25.
Seth, A., Otomo, C. and Rosen, M. K. (2006). Autoinhibition regulates cellular localization and actin assembly activity of the diaphanous-related formins FRLalpha and mDia1. *J Cell Biol* 174, 701-13.
Shimada, A., Nyitrai, M., Vetter, I. R., Kuhlmann, D., Bugyi, B., Narumiya, S., Geeves, M. A. and Wittinghofer, A. (2004). The core FH2 domain of diaphanous-related formins is an elongated actin binding protein that inhibits polymerization. *Mol Cell* 13, 511-22.
Spudich, J. A. and Watt, S. (1971). The regulation of rabbit skeletal muscle contraction. I. Biochemical studies of the interaction of the tropomyosin-troponin complex with actin and the proteolytic fragments of myosin. *J Biol Chem* 246, 4866-71.
Stradal, T. E., Rottner, K., Disanza, A., Confalonieri, S., Innocenti, M. and Scita, G. (2004). Regulation of actin dynamics by WASP and WAVE family proteins. *Trends Cell Biol* 14, 303-11.
Wallar, B. J. and Alberts, A. S. (2003). The formins: active scaffolds that remodel the cytoskeleton. *Trends Cell Biol* 13, 435-46.
Wallar, B. J., Stropich, B. N., Schoenherr, J. A., Holman, H. A., Kitchen, S. M. and Alberts, A. S. (2006). The basic region of the diaphanous-autoregulatory domain (DAD) is required for

autoregulatory interactions with the diaphanous-related formin inhibitory domain. *J Biol Chem* 281, 4300-7.
Xu, Y., Moseley, J. B., Sagot, I., Poy, F., Pellman, D., Goode, B. L. and Eck, M. J. (2004). Crystal structures of a Formin Homology-2 domain reveal a tethered dimer architecture. *Cell* 116, 711-23.
Yonetani, A., Lustig, R. J., Moseley, J. B., Takeda, T., Goode, B. L. and Chang, F. (2008). Regulation and targeting of the fission yeast formin cdc12p in cytokinesis. *Mol Biol Cell* 19, 2208-19.
Zaoui, K., Honore, S., Isnardon, D., Braguer, D. and Badache, A. (2008). Memo-RhoA-mDia1 signaling controls microtubules, the actin network, and adhesion site formation in migrating cells. *J Cell Biol* 183, 401-8.
Zaritsky, A., Parola, A. H., Abdah, M. and Masalha, H. (1985). Homeoviscous adaptation, growth rate, and morphogenesis in bacteria. *Biophys J* 48, 337-9.

FIGURE LEGENDS

Figure 1

The N-terminal region of mDia1 contains a basic domain. (A) Schematic representation of the mDia1 domain architecture (GBD: GTPase-binding domain, DID: Diaphanous-inhibitory domain, DD: dimerization domain, CC: coiled-coil region, FH: formin homology, DAD: Diaphanous-auto-regulatory domain) and the N-terminal basic region (BD) which consists of 60 amino acids with three short basic stretches (blue). Construct N46 contains the first two basic motifs. Two synthetic peptides – peptide A and peptide B (underlined) derived from the N-terminal region were used in competition assays shown in Figure 2B. (B) Multiple alignments of the first two basic stretches of mDia1, mDia2 and DAAM1 and DAAM2.

Figure 2

The BD interacts with negatively charged phospholipids. (A) Cosedimentation assays (S: supernatant, P: pellet) revealed that GST-tagged N570, Δ12-21N570, N54 and N46 interact with lipid vesicles (48:48:4, PC/PS/PIP_2) but not the constructs ΔBDN570 and Δ12-42N570. The GST control did not bind lipid vesicles containing PC, PS and PIP_2. (B) The protein/lipid interaction of N46 requires both basic stretches because each of the synthetic peptides can completely block binding to the vesicles.

Figure 3

The mDia1 N-terminus binds PS/PIP_2 and inserts into the membrane. Constructs containing the BD quench the signals of both fluorescently labeled lipids PS (A) and PIP_2 (B). The clustering of PIP_2 by the BD (N46) was the most efficient. A protein fragment lacking the crucial residues in the BD (Δ12-42N570) showed in both cases the least lipid interaction. (C) Changes in the DPH anisotropy implied that both N570 and Δ12-42N570 inserted into the plasma membrane independent of the presence of PIP_2. N46 is apparently too short and did not show significant changes of anisotropy. (D) However, both PIP_2 and the presence of the BD in N570 boosted its insertion into the membrane. Liposomes at indicated ratios were used.

Figure 4

The basic domain is essential for recruitment of mDia1 to the plasma membrane. (A) Schematic representation of the constructs used for the transfections. The full-length and truncated mDia1 versions were expressed as EGFP fusion proteins in NIH 3T3 fibroblasts and the live cells were imaged using a LSM510 Zeiss confocal microscope. (B) Representative cells of each mutant, expressing EGFP-mDia1FL (left), EGFP-mDia1ΔDAD (middle) and EGFP-mDia1ΔBDΔDAD (right) are shown. The presence of the EGFP-mDia1ΔBDΔDAD in emerging filopodia (inset, right panel) suggests that functional formin at the barbed ends of filopodial actin filaments might be anchored in the tip complex by means of membrane independent interactions with a formin. The scale bar represents 20 µm. Depicted below are the corresponding plots showing the fluorescence intensity profiles across the plasma membrane (white boxes). (C) Percentage of cells with plasma membrane localization for each mutant is plotted as a bar chart. The error bars indicate mean standard deviation of four independent transfections. Overall EGFP-mDia1FL (n = 68), EGFP-mDia1ΔDAD (n = 88) and EGFP-mDia1ΔBDΔDAD (n = 125) cells were counted.

Figure 5

TIRF microscopy of actin filaments assembled by full-length or C-terminal fragments of mDia1. (A) Micrographs of the assembly of 1 µM ATP-actin and 0.3 µM Alexa-Fluor-488-labeled ATP-actin (488 actin) in TIRF buffer on cover slips coated with 10 nM NEM-myosin II and 400 nM of GST-mDia1-FL. Addition of 5 µM GTP-bound RhoA(V14) resulted in activation of mDia1. Addition of 1 µM PIP_2 inhibited formin-mediated actin assembly. Arrow heads indicate growing

filament barbed ends, circles mark barbed ends captured by mDia1. The asterisk highlights a representative formin-induced buckling filament. (B) Scheme of insertional assembly of monomer to a filament bound to GST-mDia1(left) and NEM-myosin-II (right). (C) Quantification of active GST-mDia1-FL molecules. For each experiment an area of 100 x 100 µm was analyzed, arrow bars show standard deviations. (D) Micrographs of the assembly of 1 µM ATP-actin and 0.3 µM 488 actin in TIRF buffer on cover slips coated with 400 nM C-terminal constitutively active constructs of mDia1. 1 µM PIP_2 liposome (48:48:4, PC/PS/PIP_2) inhibits GST-mDia1FH1FH2DAD. (E) Quantification of active mDia1FH1FH2DAD in the presence or absence of PIP_2. Error bars indicate standard deviations.

Figure 6

PIP_2 inhibits mDia1FH1FH2DAD-mediated actin assembly and induces strong clustering and membrane insertion. (A) Actin (3 µM) was polymerized in the presence of wild type mDia1FH1FH2DAD and LUVs containing increasing concentrations of PIP_2 (70:30, PC/PIP_2). The dotted grey line represents the actin control. (B) mDia1FH1FH2DAD effectively clusters PIP_2 and PS as observed by the quenching of NBD-PS and bodipy-TMR-PIP_2. (C) A profound increment in the DPH anisotropy indicates that mDia1FH1FH2DAD also inserts into the membrane with LUVs composed of PIP_2 or PS. The presence of PIP_2 in the liposome boosted the membrane insertion ability of mDia1FH1FH2DAD. Liposomes at indicated ratios were used.

Figure 7

Schematic summary of putative mDia1 regulation based on known formin activities, the data from the current study and expected reactions that still need experimental confirmation. Auto-inhibition of cytoplasmic formin occurs by the interaction of DID and DAD (step 1). Upon signal transduction GTP-bound RhoA binds to GBD, thus unfolds the protein and enables the FH2 domain to nucleate actin polymerization; at the same time the N-terminal phosphatidylserine-binding region BD establishes the contact of the putatively active formin at the plasma membrane (step 2) which will be further strengthened by the IQGAP-DID interaction (not shown). For reversible fine tuning of formin-driven actin polymerization PIP_2 clusters might be generated by an increased activity of PIP_5 kinase in response to a stimulus, leading to an inhibition of formin activity by binding to the DAD and the FH2 domain (step 3). This would keep the formin in its open but transiently inactive conformation. A GTPase-independent re-activation could rely on the degradation of PIP_2. Eventually, membrane-bound formin would return to its auto-inhibited stage after GTP hydrolysis and dissociation from the membrane. GBD: GTPase-binding domain, DID: Diaphanous-inhibitory domain, FH: formin homology, DAD: Diaphanous-auto-regulatory domain, BD: basic domain.

Figure S1

mDia1ΔDAD and mDia1ΔBDΔDAD constructs are equally active in vitro. 2 μM actin was polymerized in the presence of recombinant mDia1 constructs GST-mDia1ΔDAD (green line) and GST-mDia1ΔBDΔDAD (magenta line). The actin assembly mediated by GST-mDia1ΔBDΔDAD is identical to that of the GST-mDia1ΔDAD at the respective nanomolar concentrations. Actin control is indicated by a grey line.

Figure S2

PIP_2 inhibits RhoA induced mDia1 activity. 2 μM actin was polymerized in the presence of mDia1FH1FH2DAD (orange line). Addition of the N-terminus of mDia1 (N570) resulted in intermolecular DID/DAD inhibition (blue). Inhibition was relieved by adding constitutively active RhoA which removes N570-DID from mDia1FH1FH2DAD (green line) but this activation was inhibited in the presence (grey line) of PIP_2 (48:48:4, PC/PS/PIP_2). Actin control is indicated by a dotted grey line.

Figure S3

PIP_2 inhibits mDia2 and mDia3 mediated actin assembly. (A) 2 μM actin was polymerized in the absence of mDia2 or mDia3 (dotted grey lines). Addition of 50 nM GST-mDia2FH1FH2DAD (A) or GST-mDia3FH1FH2DAD (B) enhanced actin polymerization (orange lines), whereas polymerization was inhibited by addition of PIP_2 vesicles (76:20:4, PC/PS/PIP_2) in a dose-dependent manner (green and blue lines). mDia2 and mDia3 FH1FH2DAD mediated actin assembly was inhibited by PIP_2 at a concentration of 2 μM and 700 nM, respectively. Actin assembly mediated by both mDia fragments remained unaffected by phospholipid vesicles lacking PIP_2 (black lines).

Figure S4

mDia1DAD relieves PIP_2-mediated inhibition of FH1FH2DAD activity. The green line represents actin assembly mediated by GST-mDia1FH1FH2DAD. While PIP_2 (48:48:4, PC/PS/PIP_2) inhibited the actin assembly (blue line), the addition of increasing amounts of mDia1DAD relieved the inhibition by PIP_2 in a dose-dependent manner (yellow and magenta). mDia1DAD alone did not influence the actin assembly (dotted grey line).

A

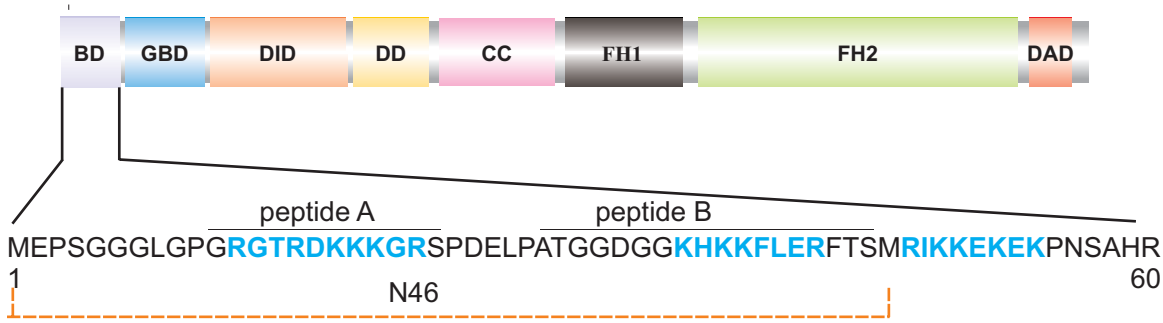

B

	First basic stretch	Second basic stretch
mDia1	G **R** G T **R** – D **K** **K** **K** G – **R** S	**K** **H** **K** **K** F – L E – **R**
mDia2	G **R** D S **K** S S **R** **R** **K** G L Q S	**K** **R** P **K** L **H** L N I **R**
DAAM1	– – – – – – – **R** **K** **R** G G **R** –	
DAAM2	– – – – – – – **R** **K** **R** S P **H** –	

Ramalingam et al., Figure 1

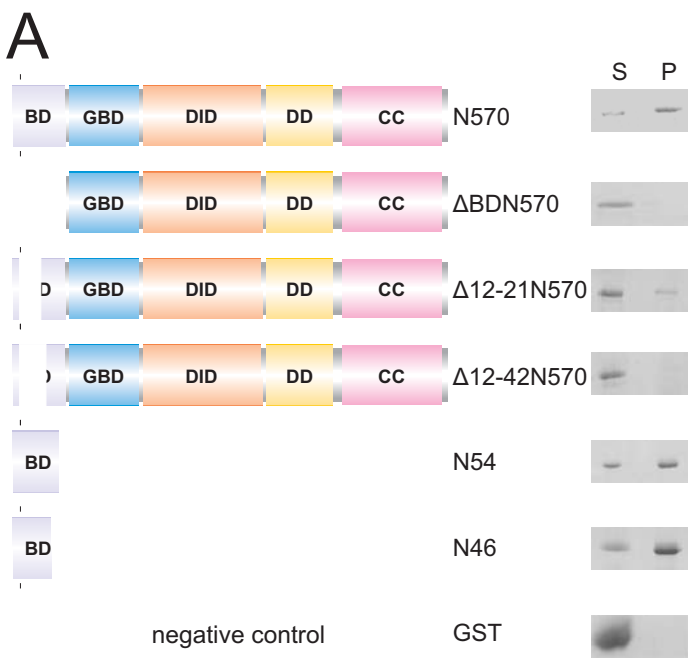

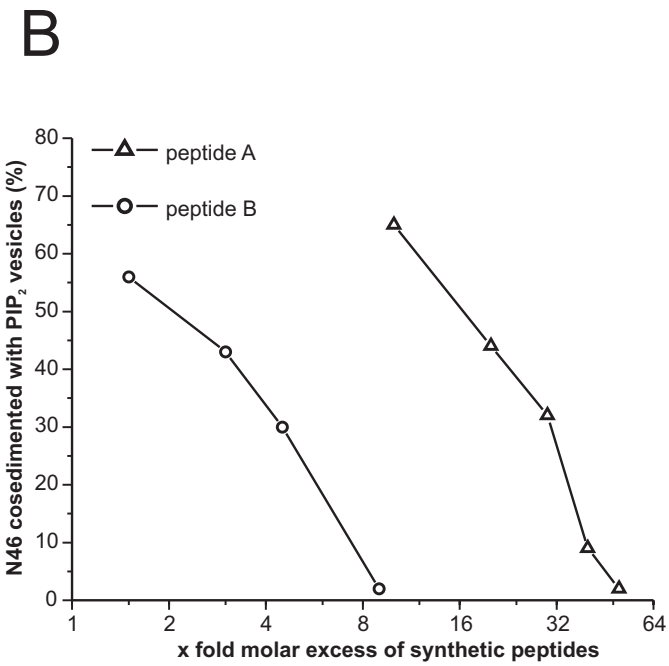

Ramalingam et al., Figure 2

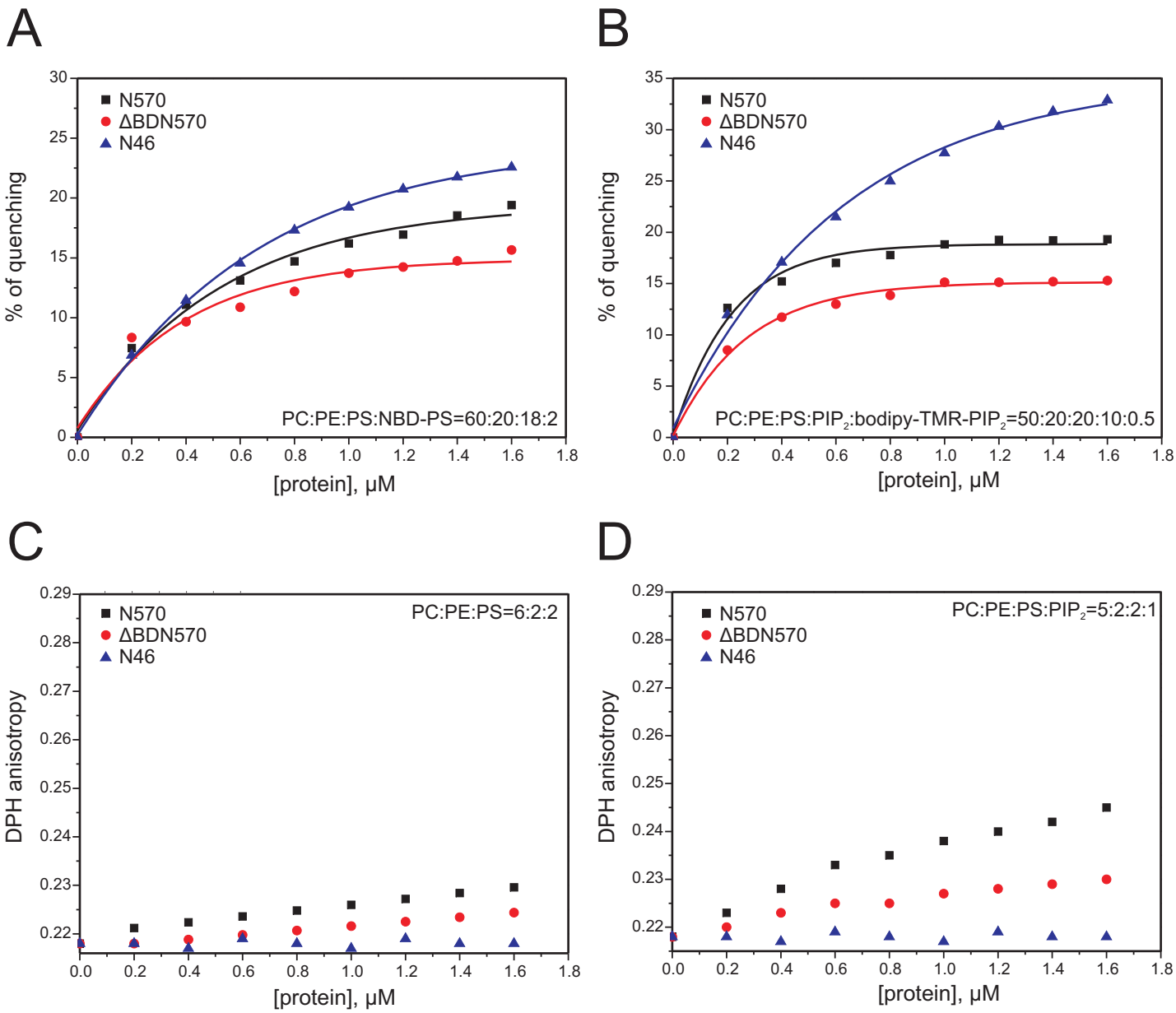

Ramalingam et al., Figure 3

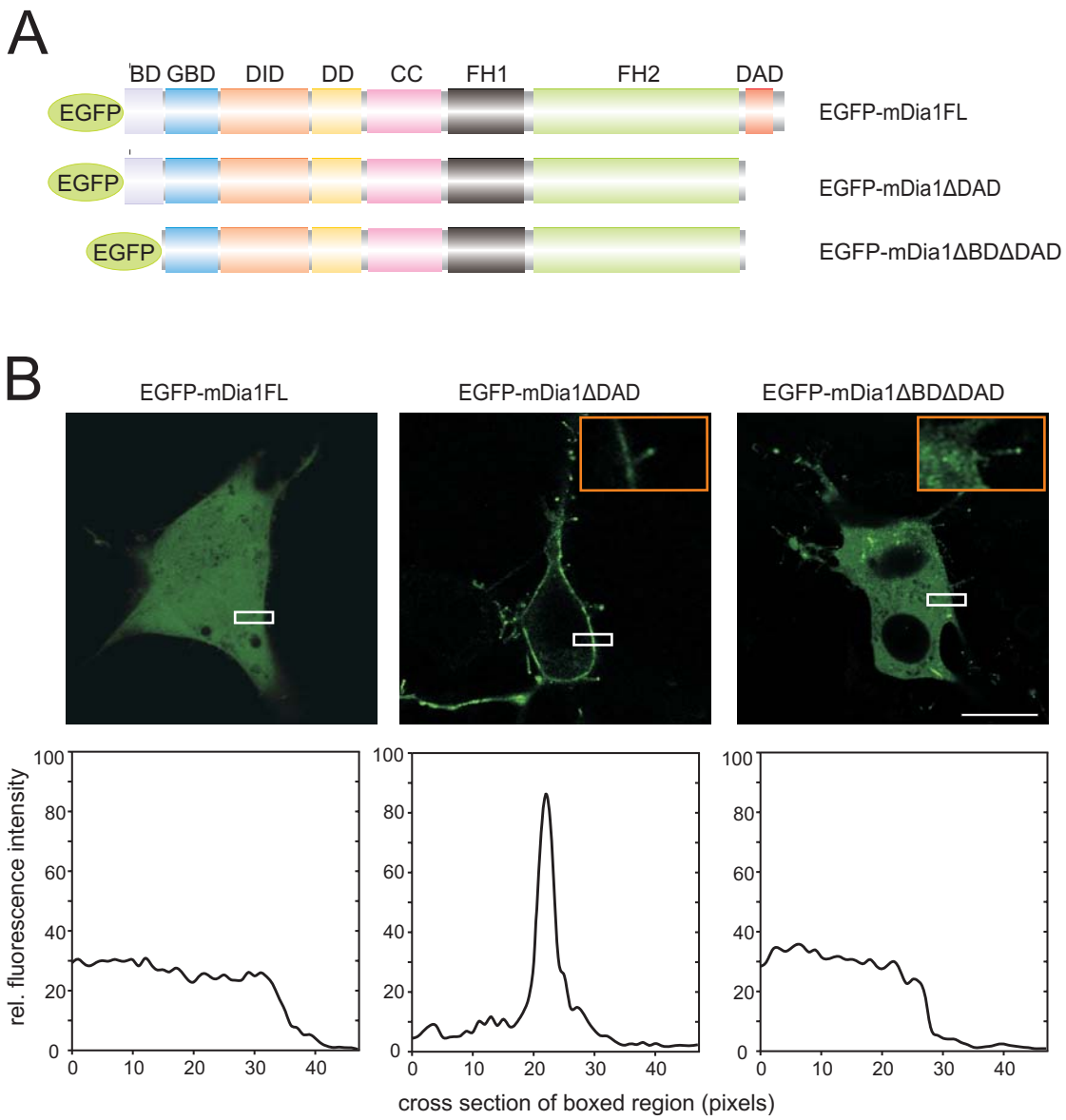

Ramalingam et al., Figure 4

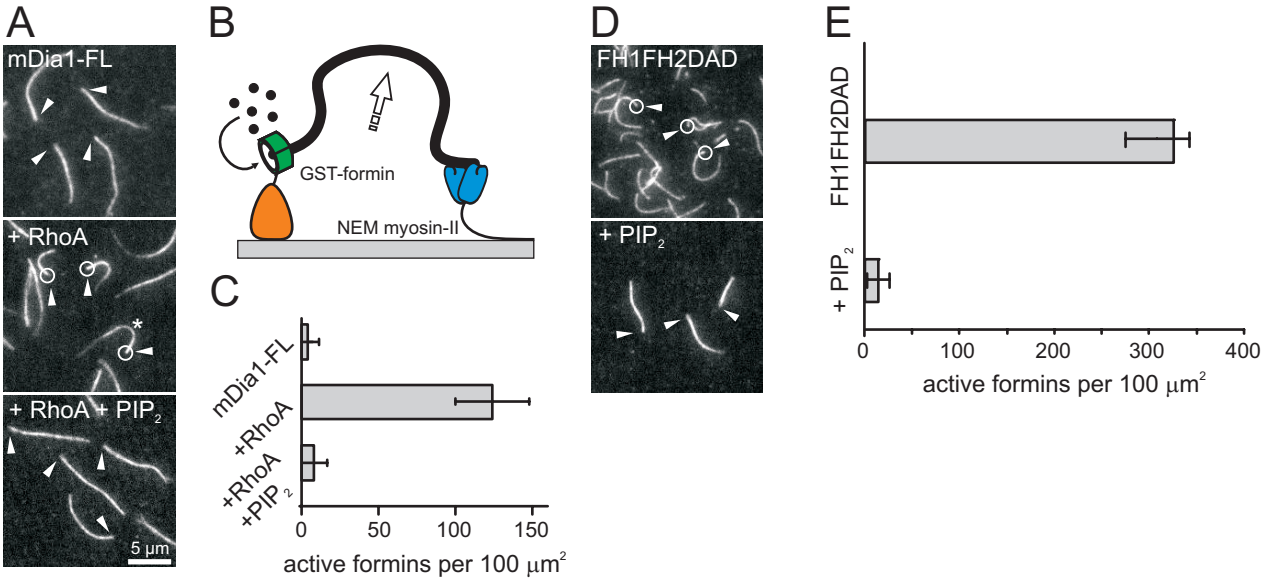

Ramalingam et al., Figure 5

A

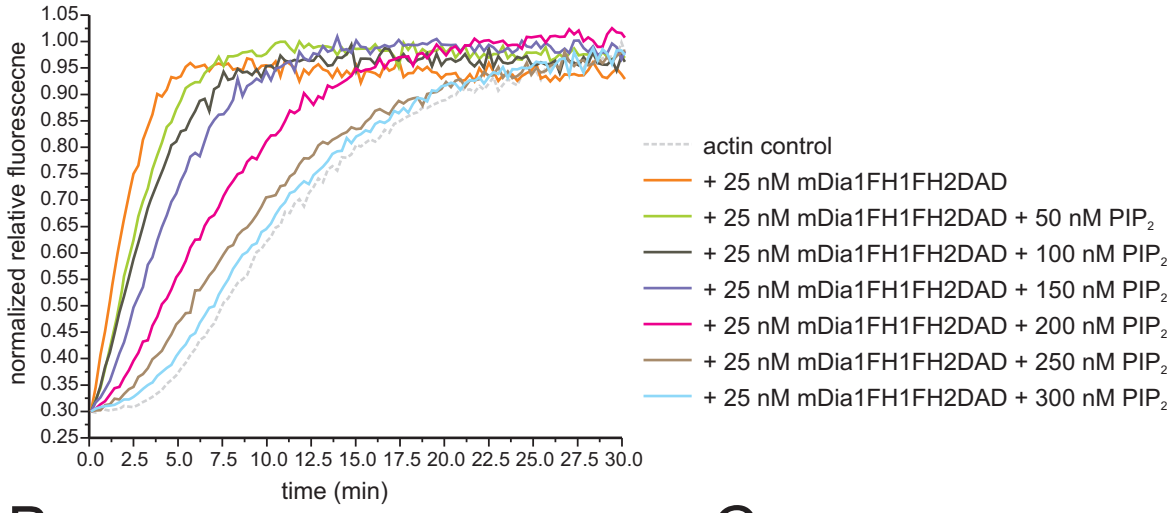

B

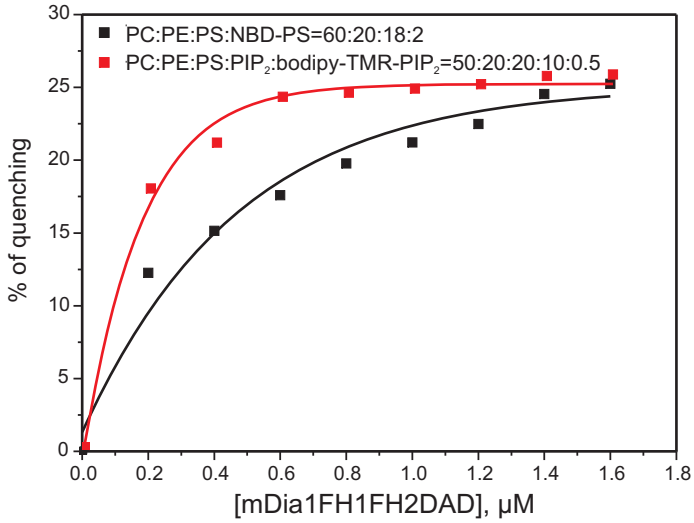

C

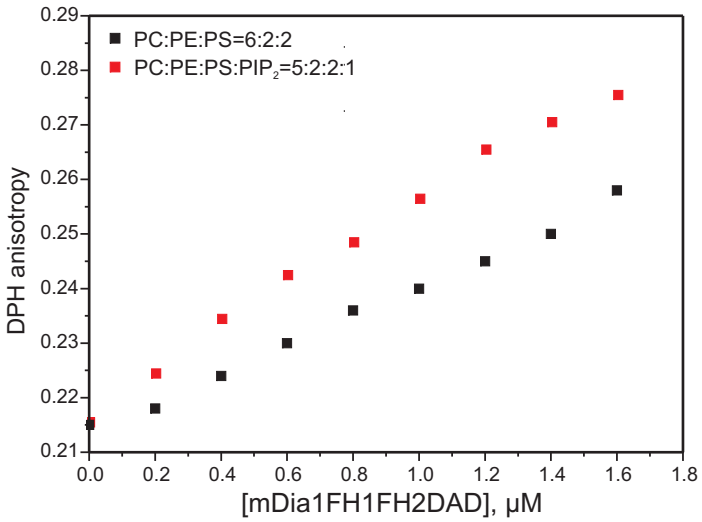

Ramalingam et al., Figure 6

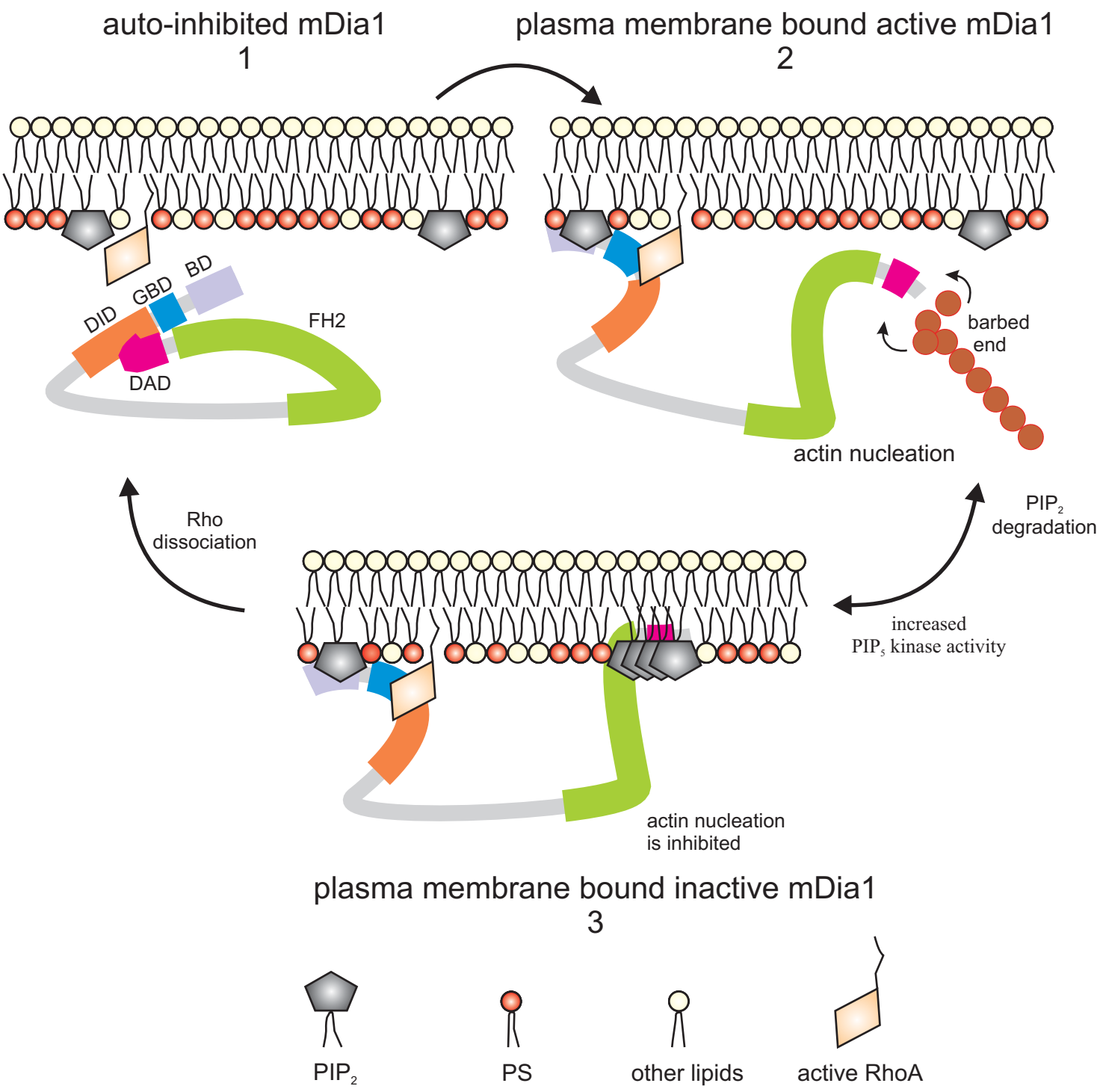

Ramalingam et al., Figure 7

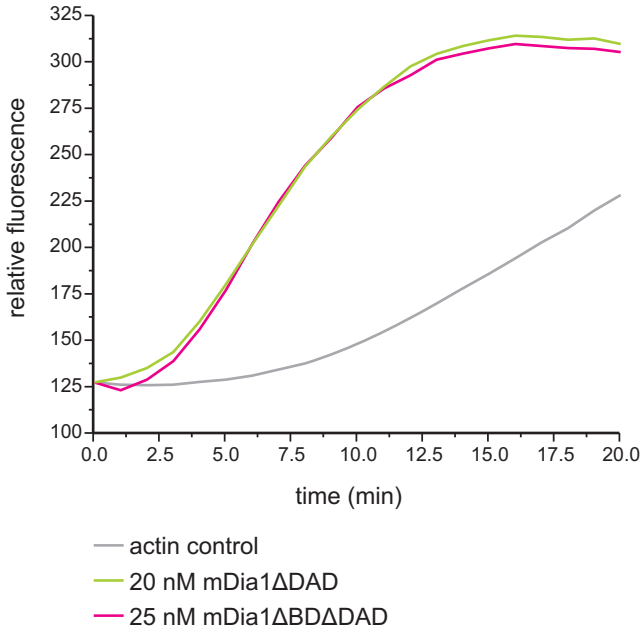

Ramalingam et al., Figure S1

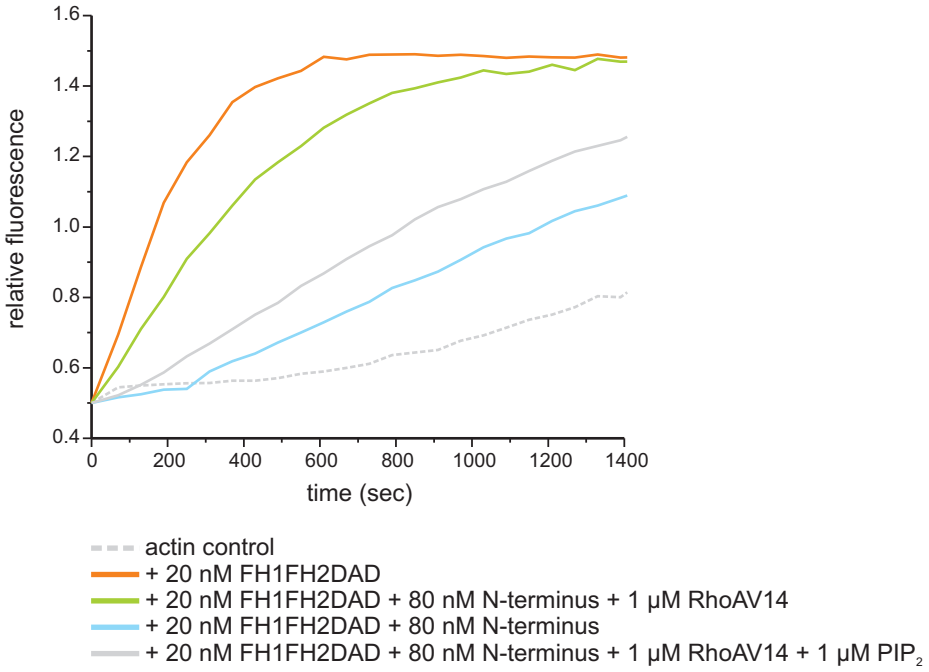

Ramalingam et al. Figure S2

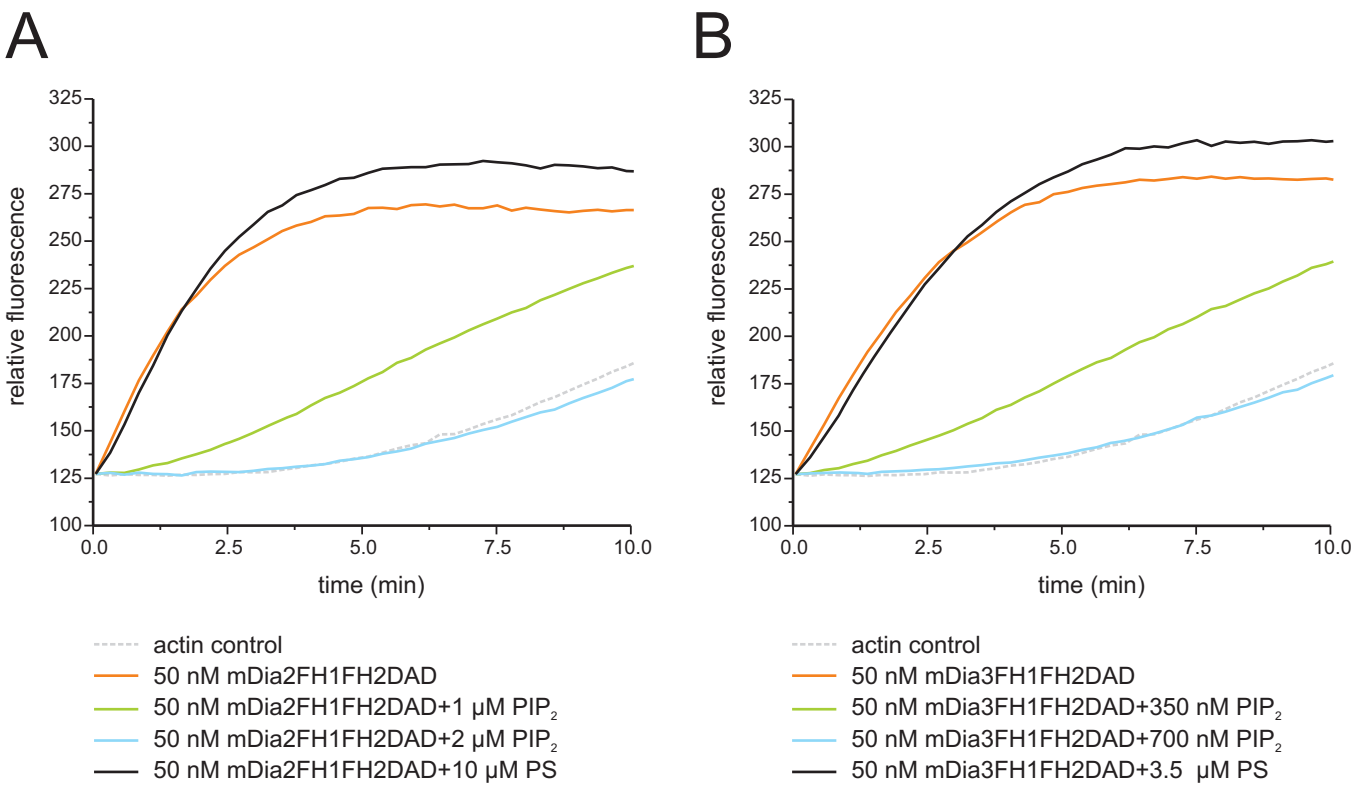

Ramalingam et al., Figure S3

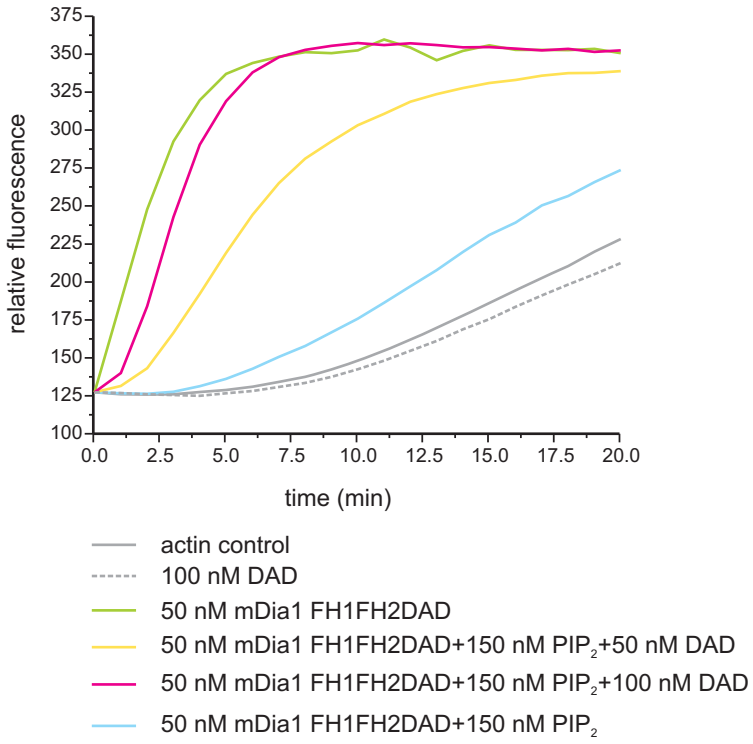

Ramalingam et al., Figure S4